iScience

CellPress
OPEN ACCESS

Review

Clinical applications of nanoprobes of high-resolution *in vivo* imaging

Shuning Kong,[1] Hua Liu,[1,2] Yue Zhang,[1,2] Jiang Fan,[1,*] and Wei Huang[1,*]
[1]Department of Thoracic Surgery, Shanghai General Hospital, Shanghai Jiao Tong University School of Medicine, Shanghai, China
[2]These authors contributed equally
*Correspondence: fan_jiang@sjtu.edu.cn (J.F.), wei.huang@shgh.cn (W.H.)
https://doi.org/10.1016/j.isci.2024.111459

SUMMARY

Currently, the primary imaging methods used in clinical diagnosis are X-ray, computed tomography (CT), ultrasound, magnetic resonance imaging (MRI), PET-CT, etc. The sensitivity and accuracy of these imaging methods bring many difficulties in clinical diagnosis; at the same time, CT, X-ray, PET-CT, etc. can cause radiation to the human body; some invasive operations of the gold standard bring much pain to the patients. Some of these tests are costly and do not allow real-time *in vivo* imaging (IVI). For these reasons, a new field of nanoprobes is gradually being developed in the clinical direction. Nanoprobes are known for their noninvasive, highly sensitive, real-time IVI and can even be expanded to intracellular imaging. This paper introduces the mainstream nanomaterial probes and reviews them regarding imaging means, imaging principles, biosafety, and clinical application effects.

INTRODUCTION

In clinical practice, medical diagnosis primarily involves laboratory tests in the clinical pathology department, imaging examinations in the radiology department, pathological biopsies or intraoperative pathological biopsies, and genetic testing. However, clinical physicians need to consider multiple factors during the diagnosis and treatment process, including cost-effectiveness, accuracy, invasiveness, and time constraints. Therefore, there is an urgent need to explore efficient, non-invasive, and precise diagnostic and therapeutic methods.

Currently, nanoprobes have attracted the attention of clinical physicians and scientists in the field of medical materials due to their relatively accurate diagnostic and therapeutic capabilities, as well as their ability to perform non-invasive in vivo imaging (IVI), and there are already *in vivo* applications for detecting atherosclerotic plaque, Silica and Silicon materials, gastric acid, or even adenosine triphosphate.[1–6] This proves that current technology can detect materials at the single-cell and subcellular levels that provide new hope for precision medicine in modern clinical practice. Significant progress has been made in live imaging by using nanoprobes, and research in this area is ongoing. However, there are also many challenges to overcome, such as the potential accumulation of probes in the body and the issue of whether they can be excreted by the liver or kidneys.[7,8]

Nevertheless, researchers are actively exploring the biological safety of nanoprobes. Currently, cell viability tests after the application of probes in cell culture show a basic level of over 80%. Therefore, the application of nanoprobes in IVI still holds great promise.

Presently, the forefront nanoprobes include those operating within the NIR-II spectrum, surface-enhanced Raman scattering (SERS) probes, DNA probes, etc. Among these, NIR-II spectrum probes exhibit diverse fluorescent markers for various bio-imaging applications, facilitated by distinct delivery and surface encapsulation techniques. However, all types of probes remain experimental and await translation into clinical diagnostic or therapeutic settings. Fluorescent markers comprise organic and inorganic dyes that emit fluorescence during *in vivo* fluorescence imaging. Organic dyes encompass aggregation-induced emission (AIE),[9] donor-acceptor-donor (D-A-D) dyes, indocyanine green (ICG) dyes, semiconductor polymer nanoparticles (SPNs), and porphyrin dyes, among others, offering high sensitivity and contrast for *in vivo* bio-imaging. And recently an unprecedented research about AIE open a new door for detecting the tumor and give us new hopes to realize precise treatment.[10] Nonetheless, they encounter limitations such as low energy transfer efficiency, poor visible emission, low photostability, and complex preparation processes.[9,11–14] Inorganic dyes include rare earth nanoparticles, carbon nanotubes, lithium nanoparticles, quantum dots (QDs), and gold nanoparticles that are deemed the most biocompatible and promising for clinical applications (Figure 1).

However, the biosafety and stability of other inorganic probes necessitate ongoing exploration. Notably, certain QDs probes have demonstrated good biosafety, whereas rare earth nanoparticles exhibit poor biosafety profiles.[15] Thus, there is a pressing need to develop biologically safe and stable nanoprobes. Delivery methods encompass liposome encapsulation, microbubble delivery, nanocellular micelles, and protein encapsulation techniques. Some rare encapsulation materials also show marvel effects, such as transferrin, BSA, etc.[15–17] Surface treatment techniques involve antibody coupling, aptamer, peptide, polyethylene glycol, and cell membrane surface encapsulation.

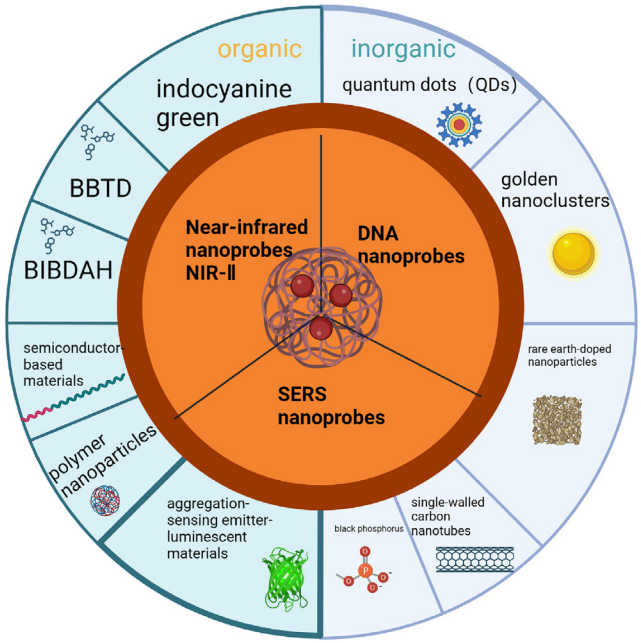

Figure 1. Three types of nanoprobes and their trackers

Employing these techniques, nanoprobes strive to advance high-resolution real-time IVI technology.[12] DNA probes primarily serve to investigate cellular-level functions, constructed with backbones, i-motifs, ligands, DNA enzymes, and other components. Current research, primarily focused on MCF-7 cells, enables probing at the microscopic level of the cell membrane, Zn^{2+} ion,[18–26] and intriguingly, functioning as voltage clamps to investigate ion flow in sodium-potassium pumps at the single-cell level. Nanoprobes harbor immense potential for future clinical applications. SERS probes, characterized by high sensitivity, facilitate the study of ion channels on cell surfaces and cell identification at varying pH values, thus heralding an emerging field for future development. We primarily focus on the current applications of near-infrared (NIR) nanoprobes, DNA probes, and SERS probes in the IVI area, presenting the latest advancements in their utilization and offer deliberations for their clinical translation.

NEAR-INFRARED NANOPROBES (NIR-II)

NIR nanoprobes represent a prevalent choice for IVI: I, II, and III. Among these, NIR-II, particularly emitting wavelength within the 1,000–2,000 nm range, stands out as the most common.[27,28] NIR-II further subdivides into a and b.[27,28] This technique is mainly used in the clinical identification of lymph nodes,[29–32] tumors, vascular anastomosis sites,[33,34] anatomical structure etc. (Figure 2). Usually, the fluorescent tracker (for example, indocyanine green [ICG] dyes) is dissolved in sterile water or saline water, then being injected through intravenous/ureteral catheter[35] (Figure 3). Presently, a diverse array of NIR-II luminescent trackers have emerged, encompassing entities such as indocyanine green, benzothiadiazole (BBTD), butyl dibenzyl aminocyclopentene, semiconductor-based materials, polymer nanoparticles, and aggregation-sensing emitter-luminescent materials, among others. Additionally, inorganic luminescent trackers, including single-walled carbon nanotubes, black phosphorus, rare earth-doped nanoparticles, golden nanoclusters, and quantum dots, have been developed.[12,36,37] Among organic luminescent materials, NIR-II imaging based on ICG is a conventional modality. However, challenges arise from the accumulation of certain coupling agents in metabolic organs, prompting the need for

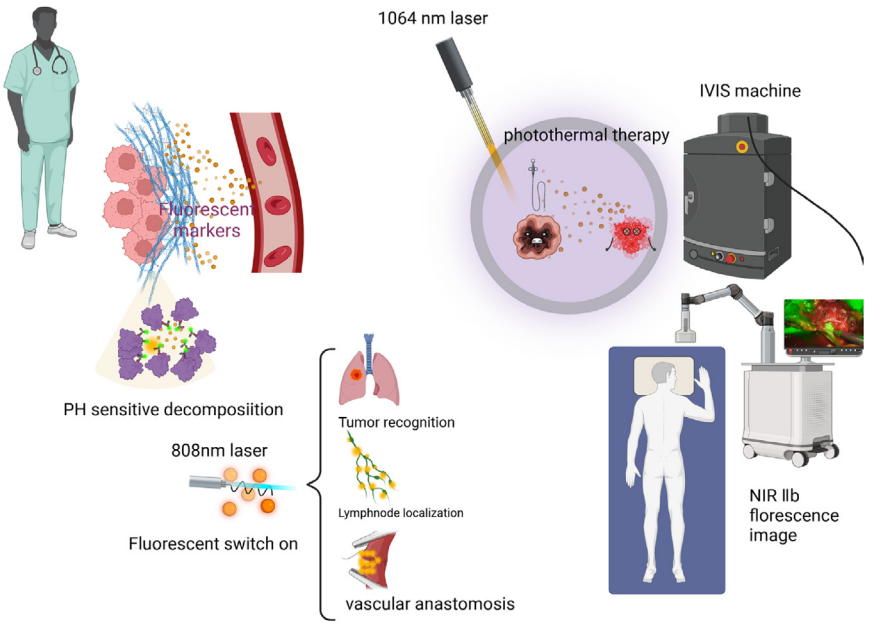

Figure 2. NIR-II applications in clinical cases

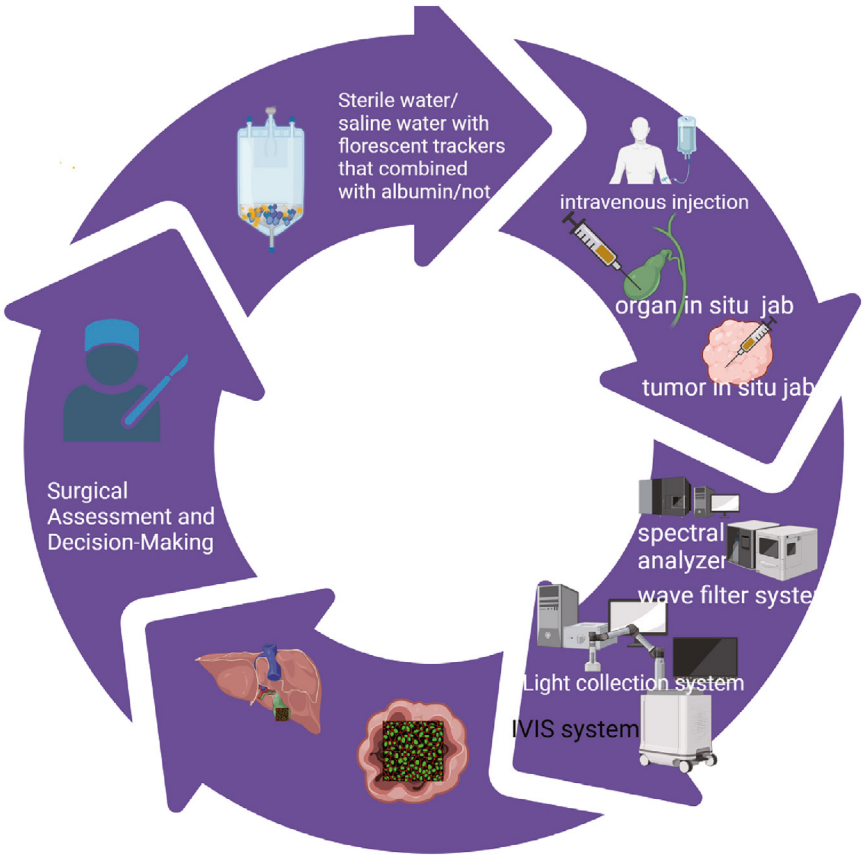

Figure 3. Steps of application of NIR-II nanoprobes

enhancements and innovations in ICG luminescent-material-based nanoprobes. In this context, transferrin emerges as one of the analogs of ICG luminescent materials, offering potential solutions.[16,38–40] Numerous meticulous research endeavors have been undertaken to engineer NIR-II fluorescent probes utilizing BBTD-derived D-A-D frameworks. These BBTD frameworks exhibit notable characteristics such as high photostability and large Stokes shifts, enabling the realization of high-performance NIR-II fluorescence imaging. This advancement encompasses enhanced imaging sensitivity and contrast, thereby offering substantial benefits for biomedical imaging applications.[11] Simultaneously, inorganic luminescent materials such as upconversion nanomaterials (UCNPs) are frequently employed. UCNP offers advantages such as mitigating background interference from endogenous cellular fluorophores, reducing the risk of photodamage to biological samples, and enhancing tissue penetration depth. These properties have made UCNP a prevalent choice in probe research.[15,41] Furthermore, golden nanoclusters are highly regarded as luminescent materials suitable for clinical applications, primarily owing to their low biotoxicity. Their exceptional photothermal conversion efficiency and customizable NIR absorption make them extensively utilized in NIR imaging endeavors.[15,27] NIR-II probes have lower photon scattering, higher resolution and sensitivity, and higher SBR compared to the limitations of the earlier NIR-I probe. Resolution and sensitivity, high SBR ratio, and deep tissue penetration[11,12,36] also overcome visible light imaging probe observation limitations. Furthermore, the advantages of NIR-IIb (1,500–1,700 nm) over NIR-IIa (1,300–1,400 nm)[42] are particularly pronounced. NIR-IIb exhibits reduced fluorophore density, diminished light scattering, and decreased absorption effects from endogenous chromophores, thereby enhancing imaging quality (Table 1) (Figure 4[42]).

NIR nanoprobes are commonly combined with photoacoustic (PA) imaging to enable fluorescence imaging with ultra-high spatial resolution and high contrast.[16] Conversely, their integration with three-dimensional multispectral PA tomography (3D MSOT) enables the visualization of disease sites, such as metastatic lesions in lymph nodes, by providing comprehensive three-dimensional spatial information.[7,45] The construction of a nanoprobe entails the incorporation of biosensors for signal imaging, with Förster resonance energy transfer (FRET) emerging as the most prevalent technique in medical imaging applications.

Table 1. The main pros and cons of the NIR-II imaging

NIR-II advantages	Drawbacks
Effectively eliminates background luminescence interference in biological systems[13]	–
NIR-II fluorescence imaging has been shown to have high performance, including improved imaging sensitivity and contrast, which facilitates biomedical imaging[38]	–
Deep tissue penetration, low autofluorescence, and high contrast-to-noise ratio[43,44]	Poor aqueous solubility of most drugs and low diagnostic specificity and sensitivity for the target of interest

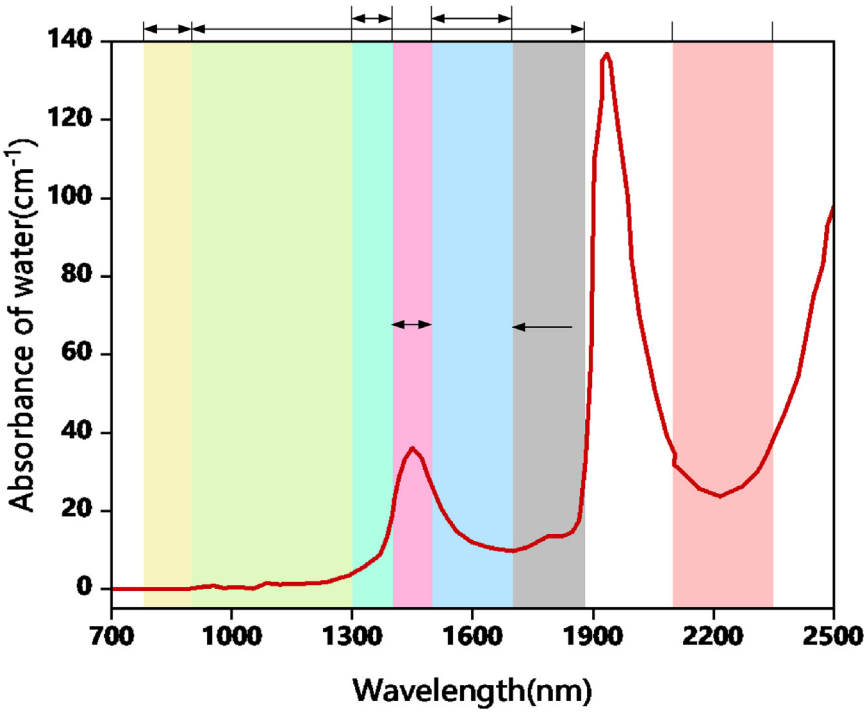

Figure 4. Different absorbance of water during different wavelengths

We can see the absorbance of water has a slice increase in the wavelength of NIR-II.

FRET employs a non-radiative mechanism where the photon energy from an excited fluorophore (donor) is transferred to another nearby fluorophore (acceptor) when donor and acceptor are near (1–10 nm). This technique enables the visualization of molecular interactions between two protein components beyond the resolution limit of optical microscopy. Additionally, luminescence resonance energy transfer (LRET) and excitation ratiometric nano detectors are utilized for specific target sensing, further enhancing the versatility of nanoprobe-based imaging methodologies.[41,46] NIR imaging is frequently used for *in vivo* bioluminescence imaging (IVIS systems) and *in vivo* fluorescence imaging for diagnostic purposes, with potential for future noninvasive imaging applications (Figure 3). Our review encompasses current clinical applications of developed probes, offering insights into the prospective utilization of nanoprobes in clinical diagnostic imaging.

Presently, the clinical applications of NIR-II imaging are classified into several categories, including intraoperative navigation, lymph node metastasis monitoring, liver injury and inflammatory response detection, and identification of tumor components based on the tumor-specific microenvironment. This microenvironment often comprises characteristics such as ATP overexpression, acidic pH, hypoxia, elevated levels of reactive oxygen species (ROS), and enzyme overexpression.[25] Another emerging research approach reveals the crucial role of microRNA in discriminating between tumor and normal tissue during imaging. Specifically, microRNA probes offer a non-destructive means of distinguishing between different types of tumor cells. For instance, fluorescence intensity measurements during imaging indicate higher intensity in A549 cells compared to HeLa cells and other cell types. However, the fluorescence intensity of microRNA probes for tumor detection exhibits variability across different tumor cell types,[47] which brings new ideas for future exploration of noninvasive tumor diagnosis.[47] The biosafety and biocompatibility of NIR-II probes have become focal points of discussion within the contemporary materials community.[38,48–53] In the development of such probes, it is essential to initially elucidate the probe construction process. Subsequently, assessing the impact of adding exciters in mouse models becomes imperative. Furthermore, a thorough evaluation of the probe's biotoxicity is warranted, along with considerations for pharmacokinetics and clearance methods.[12] The most prevalent assay involves assessing cell viability, with the option of performing HE staining on tissue sections. A control group was established to further corroborate the effectiveness of the inhibitors alongside the exciters. Currently, the most common material is Ag in the NIR-II area and is usually encapsulated by SIO2 or any other inorganic material. The table below outlines the Ag nanoprobes' clinical applications of *in vivo* probe construction over the past 5 years (Table 2).

ICG dye

ICG fluorescent trackers represent the most extensively utilized and traditional class within the NIR-II field. Nonetheless, it encounters challenges such as severe background signal interference, altered spectral properties, a narrow imaging window, and limited penetration depths, including issues like severe photobleaching.[14,16,39,43] ICGs necessitate coupling with various molecules to achieve clinical applicability. Although literature reports indicate their utilization in cancer staging and lymphatic drainage imaging, conflicting opinions exist. Some articles suggest ICG's effectiveness in identifying the lymph node itself, whereas others argue that it cannot determine whether the lymph node is metastatic.[43] The following table summarizes ICG dye modifications and their analogs and their imaging advantages within the last 5 years (Table 3).

Inorganic QD quantum dot tracker

Quantum dots are prevalent trackers in the field of nanoprobes, utilized across various applications. They possess the capability to absorb photons and subsequently emit them at diverse wavelengths. Quantum dots offer several advantages, including a substantial absorption coefficient, a narrow and adjustable emission spectrum based on size, a wide spectral window spanning from UV to IR, a prolonged fluorescence lifetime exceeding 10 ns, as well as robust optical and chemical stability.[12,40]

Table 2. The main application of Ag nanoprobes and the new explorations of creative nanoprobes in the NIR-II area

Trigger/Biomarker	Probe type	Clinical applications
Ag2S iodide nanoparticle	Upconversion luminescent nanoprobe (UCNP) near-infrared fluorescent Ag2S nanodots (NDS), AU-CU955 nanoparticles UCNPs@SiO2-Ag2S	*In vivo* pH sensing and imaging (tumors)
H2[12]	Bimodal second NIR/photoacoustic smart nanoprobes SiO2@Ag	Highly specific imaging of colorectal cancer
HClO[54]	Ag2Te@Ag2S core-shell QDs	Arthritis and peritonitis
H2S[55]	NIR-II optical properties of NaYF4:Gd/Yb/Er@NaYF4:Yb@SiO2@Ag by adding S2−	Metformin-induced liver injury

Different kinds of probes have different excitation conditions, depending on PH and different chemicals. These different biomarkers provide a lot of thinking for the clinical diagnostic process. The use of different probes in the clinic is also different and can be used for tumor lymph node biopsy and tumor microenvironmental detection, which are at the microscopic level or even subcellular structure level of the non-invasive *in vivo* biomarker imaging, so for the future of the clinical precision therapy to provide a new choice and thinking.

Currently, the commonly used quantum dot coupling agents are PbS/CDS/ZnS, CdSe/ZnS, CdTe/CDS, and CdTe.[40,45] Previous studies in the literature have demonstrated the utility of quantum dots in various applications, including cellular imaging of HER2-positive breast cancer, imaging of lymph node metastasis, and intraoperative navigation for prostate cancer. Biosafety assessments confirmed a cell survival rate of 80%, indicating the potential of inorganic quantum dot tracing for future clinical research endeavors. PSMA-QD655 is a deep-tissue imaging agent that is used for intraoperative navigation. Krishnan et al. have reported this technology in prostate cancer. This nanoprobe is designed and synthesized by coupling functionalized amino-PEG quantum dots (QDs) to DUPA-targeted peptide constructs with heterobifunctional linkers. Interestingly, this nanoprobe is distinct from typical ICG fluorescent navigation that is used mainly for navigation of lymph nodes and leaves the potential for inorganic trackers that are less likely to accumulate in metabolic organs.[56–60] Furthermore, two kinds of quantum dots attract our attention, Ag2Te@Ag2S core-shell QDs that can detect arthritis and peritonitis by sensing the density of HClO. Quantum dots release positive ions to present them to Ag, and NaBH4 reduces the Ag ion to stimulate fluorescence quenching. Then, after sensing the HClO that exists in arthritis and peritonitis patients, the QDs restore to remit, counteracting the fluorescence quenching effect.[54] This delicate design qualifies the extent of this type of disease and has the specific index to evaluate.[45] Another nanoprobe MnCuInS/ZnS@BSA-Ab ingeniously combines QDs with BSA and encapsulates certain chemical groups to characteristically combine with HER2 antibodies.[40] Coincidentally, Chen et al. also use BSA as encapsulation for lymphatic metastasis visualization for surgery. This tricyanofuran heteroanthracene alanine nanoprobe X-APN@BSA sense aminopeptidase N to be activated for photoacoustic/NIR-II fluorescence dual-mode imaging to track lymphatic metastases and guide tumor resection procedures.[7,45]

Golden nanoparticles

The main difficulties faced by small molecule trackers at present are poor biocompatibility, easy aggregation in metabolic organs, poor water solubility, etc.[39] Gold nanoparticle tracker probes are considered to be the most appropriate nanoprobes to apply to bioimaging because of their excellent biosafety, high sensitivity, and real-time monitoring.[15,27] In addition to possessing excellent photostability and chemical stability akin to quantum dots, gold nanoparticles offer numerous advantages, including straightforward synthesis, ultra-small size, substantial Stokes shift, and good water solubility. However, it is important to consider economic costs, as well as the fact that the absorption spectrum

Table 3. The ICG dye and its analogs applied for NIR-II imaging explorations

	Cypate (Cy@aft) apolipoprotein coupling[16]	Tumor imaging (PTT enabling tumor RF ablation)	Activity targeting and long-circulation properties facilitate accurate tumor visualization over long windows
Folate receptor alpha[38]	Bimodal nanoprobe indocyanine green (ICG) dye and DOTA chelator coupling	Fluorescence imaging and image-guided surgery for glioblastoma	–
Thermosensitive, lipopolysaccharide (LPS) endotoxin[39]		Rheumatoid arthritis	With high sensitivity, specificity, and signal-to-background ratio (SBR)
VEGFR-3[17]	TMVP1-ICG-NPs	Sentinel lymph node tumor metastasis	–

ICG dyes are currently the most widely used organic dyes, but due to some of their biotoxicity and other drawbacks, people continue to explore the emerging field of probes. ICG dyes are still more traditional and widely used, so we summarize some of the last five years of ICG dyes and their analog nanoprobes.

of gold nanorods primarily falls within the NIR-I region. Consequently, a current research focus and challenge involve red-shifting their absorption to the NIR-II region. Furthermore, gold nanomaterials exhibit ease of integration with DNA probes, as elaborated upon later.[27] We conclude the gold nanoprobes depicted by recent articles are applied in tumors' *in vivo* pH sensing and imaging, predict heart failure, and monitor the potential for second proximal gastric acid and even cranial imaging,[13–15,27] which are separately triggered by HCL, phosphoprotein (PLN) (a neuropeptide present in the sarcoplasmic reticulum [SR] of cardiac myocytes), and special luminous metal material. Presently, gold nanoparticles find clinical applications in microRNA imaging and encapsulation within dopamine for gastric acid detection. Notably, the nanoprobe designed for gastric acid detection can be administered directly via gastric gavage, exhibiting favorable characteristics such as good biosafety, rapid excretion, and absence of accumulation in metabolizing organs. This nanoprobe is composed of Au NCs@PDA-MB (PDA: dopamine and MB: methylene blue). Gold nanoprobe is triggered by glutathione and enfolded by PDA, then loaded MB on the surface of the nanoprobe; this entails the sensitivity, high-response speed high SBR, and better biosafety and enables this nanoprobe to accurately sense the HCl density.[15] Gold nanoprobes are also explored in the neurosurgery department, but it was only limited to the laboratory animal science area. Nanoprobes detecting mouse cranial nerve are created, which combine GNR (Au nanorods enfolded by SIO2) with P dots. However, this kind of nanoprobe still has limitations. Even though, NIR-II fluorescence imaging provides a valuable method for accurately visualizing biological structures deep within the body. Unfortunately, most NIR-II fluorophores suffer from low absorbance and low quantum yield (QY) in cranial nerve detection.[14] Another literature has used glutathione-induced change of MnO2 to Mn2+ and, thus, *in situ* aggregation of gold nanoparticles for imaging of tumors.[27] When it comes to heart failure, there is no evident golden standard to diagnose except for detecting BNP or NT pro-BNP. We usually do not make biopsies to identify the heart condition in the initial diagnosis and treatment process because it is invasive, so gold nanoprobes become a potential choice. Because it is triggered by the phosphoprotein that only exists in heart failure patient that specifies the accuracy of our diagnosis, the composition of this nanoprobe is the functionalization of thiol-modified DNA short strand (C-strand) combined with gold nanoparticles that have specific roles for detecting and imaging phosphoprotein micro peptides in cardiomyocytes.[61]

UCNP

Upconversion luminescence absorbs two or more low-energy photons and emits one high-energy photon.[41] Upconversion luminescent materials are categorized into four main groups: lanthanide-doped rare-earth UCNPs, single-photon frequency upconversion luminescence (FUCL), triplet-triplet annihilation (TTA), and two-photon absorption upconversion luminescence (TPA).[21–24] Rare-earth upconversion nanomaterials, which include rare-earth elements, offer numerous advantages for probe construction and fluorescence imaging. These advantages comprise significant anti-Stokes shifts, excellent photostability, absence of photobleaching, high tissue permeability, and minimal photodamage. UCNPs can effectively detect deep-tissue microRNAs through NIR reactivity, although challenges persist regarding their bioadaptation. Despite the adaptability challenge, an ongoing exploration into the utilization of UCNP materials for IVI with fluorescent probes is underway, leveraging the LRET process mentioned earlier. Successful surface assembly of pyranonitrile dyes on lanthanide upconverted nanofluorescent powders (UCNPs) has been reported, indicating the potential for UCNPs in future clinical applications.[23,41,62–64] UCNP is most commonly composed of NaYF4:Yb,Er encapsulated by silica,[36,47,55] and most UCNPs are currently used mainly for microRNA detection. UCNPs are extensively applied in material areas and cooperate with bioscience technology. By sensing β-gal, DCM-β-Gal UCNPs upconversion nanoprobes modified with pyranonitrile nanoprobe are used for ovarian cancer tracing changes in β-GAL activity in living cells (293T and SKOV-3 cells).[41] Another interesting nanoprobe is a dumbbell-shaped UCNP-loaded UV-responsive DNA dumbbell-like structure probe (PH1) that senses ultraviolet rays and microRNA to emit green fluorescence to detect the density of the tumor area.[47]

Rare-earth nanoprobes

This type of nanoprobe faces a lot of challenges because it will cause damage to the human body. Thus, it is less likely to apply to clinical conditions,[43] but due to its smaller apparent diameter/width and higher SBR, scientists still try to exploit this area. Based on approval of the biosafety of these nanoprobes, we summarize two types of rare-earth nanoprobes in breast cancer detection, NaErF4@NaYF4 NIR-IIb nanoprobes (ErNPs). Rare-earth nanoprobes modified ErNPs with balisafopeptide (ErNPs@POL6326) to detect breast cancer sentinel lymph node metastasis. Balisafopeptide plays as a biomarker and is a peptide antagonist of the chemokine receptor CXCR4.Rho@ErNPs@POL6326. Even though authors verified the biosafety of this nanoprobe, they also admitted that they may have some hindering risks during the process of fluorescence quenching and restoration.[43] Another instance is the rare-earth core-shell nanoprobe NaGdF4: 5% ND@NaLuF4 depicted by Wei et al. They prove the cell viability is over 80% and the hemolysis is less than 5%.[65] Interestingly, Zhu reported that nanoprobes that use rare-earth dye can detect bacterial infection. TPEO-820-dye-sensitized rare-earth doped nanoprobes (RENPs) with a ZIF-8 layer incorporating the photochemically triggered nitric oxide donor CysNO to detect MARSA infection. This provides a new area for clinical operators to evaluate healing of the patients in their convalescent phase.[66] All in all, the resolution of this material is critical; excluding vital drawbacks, rare-earth nanoprobes still hold bright prospects.

Other nanoprobes

Except for the aforementioned nanoprobes, some burgeoning nanoprobes are also being explored. ROS nanoprobes, for example, are booming in the material area. RHyLI nanoprobes allow real-time quantitative measurement and monitoring of tumor hypoxia during radiation therapy sessions. It is a non-radiation and low-cost device and can even detect the oxygen level of the vessel.[67] Then, there are some rare nanoprobes, all used in tumor detection; glyoxal-triggered FRET-based peptide

Table 4. Other nanoprobes of different clinical applications

Trigger/Biomarker	Probe type	Clinical applications
H202[7]	Benzothiadiazole core nanoprobe BTPE-NO2@F127	Interstitial cystitis and liver ischemia-reperfusion injury
Methylglyoxal[11]	MGSLNP organic magnesium oxide probe TDTCD	Type 2 diabetes mellitus (T2D)
Nitroreductase[8]	Pep(peptidized)/BDP-NO2@Lip. The nanoprobe is a liposome-based nanostructure that is functionalized by a peptide (GGGGDRVYIHPF)	Myocardial hypoxia visualization
AIE-activated aggregation-induced emission[9]	A total of four acrylonitrile-based aggregation-induced emission (AIE) active two-photon (TP) fluorescent probes	Efficient deep brain vascular imaging
–	NaGdF4:Nd 5%@NaGdF4@Lips (named GdREs@Lips) liposome encapsulation	Imaging studies in a xenograft model of hepatocellular carcinoma patients have been shown
Granzyme B, semiconductor polymer (SP)[61]	Activatable semiconductor polymer nanoprobes (SPNP)	T-lymphocytes
ATP[70]	NIR@ZIF-90 was prepared by embedding a rhodamine-like near-infrared (NIR) dye in a molecular sieve imidazole backbone (ZIF-90)	Colon inflammation

nanotubes examine tumor tissue.[46] AIM-Probe, Cys(StBu)-Lys(Cy5.5)-EDA-PMA-CBT self-extinguishing fluorescent nanoparticles can sense the PH of tumor because it has low PH.[68] Wang et al. invented an "albumin−conjugate" nanoprobe. HSA-Er-RI-Cl contains serum protein erlotinib and a hypoxia-targeting heptamethine carbocyanine dye. Because it uses small molecules, it is rare in nanoprobe materials due to poor biocompatibility. Small molecule preparations are easy to accumulate in metabolic organs such as the liver and kidney. But this research uses albumin to smoothly tackle this problem. It detects subcutaneous and metastatic tumors in the HNSCC cell line and tumor tissue from the HN30 group.[69] Moreover, QT-RGD NIR-emitting organic fluorophore and two cyclic (arginine-glycine-aspartate) (CRGD) peptides are other interesting nanoprobes that are used for tumor thermotherapy, which is triggered by αvβ3 integrin.[44] A more sophisticated type of MnO2-JANUS-PPA nanoprobe is used to detect tumor immune microenvironment.[40] Except for the oncology field, there are also other nanoprobes used in different areas, which are shown in Table 4.

DNA NANOPROBE

DNA nanoprobes offer several advantages, including programmability, high molecular recognition accuracy, good biocompatibility, straightforward synthesis, easy modification functionalization, and a modular structure. In the context of DNA nanoprobes, which primarily serve as auxiliary modifiers, we compile a summary of nanoprobes incorporating DNA modifications that have been visualized under NIR and utilized in various fluorescent trackers as mentioned earlier. These DNA nanoprobes are predominantly employed for imaging within living cells and molecular imaging of cell membranes, among other applications.[18–26] The following table describes the components of DNA nanoprobes and their functions (Table 5).

The main applications of DNA nanomaterials on cell membrane surfaces are fluorescence imaging and functional modulation. In this paper, we investigated the application of DNA nanomaterials in fluorescence imaging of cell membranes.[8] Gao et al. introduced a multicolor covalent organic backbone DNA probe, where the DNA fluorescence signal is initially quenched by the probe backbone, and recognition of the aptamer restores the fluorescence signal. The construction of DNA nanoprobes necessitates a backbone and multiple modification groups to ensure probe stability. Typically, the aptamer is furnished with fluorescence signals at both ends (e.g., Cy3/Cy5). Moreover, recent studies have demonstrated the utility of DNA nanoprobes in imaging sodium-potassium pumps on cell membranes, reminiscent of the voltage clamp principle in physiological investigations. This presents promising opportunities for advancements in basic research.[71–74] Specific DNA nanoprobes from the last 5 years of research are summarized in Figure 5.

The aptamers are protein-specific binding units of receptor proteins (MUC1 is the most common) that are labeled to restore the fluorescent signal cy3/cy5,[20–23,26] DNA tetrahedral nanostructures, AuNP, etc.. I-motif is a proton recognition probe. DNAzyme is used for building sensors, similar to the aptamer, but is absorbed on skeletons, which can be used in future gene tests.[24,25,75]

DNA nanoprobes, precisely because of their specific binding ability, have a wide range of clinical application prospects. Different nanoprobes have different ways of improving their specific binding ability, among which are the application of freezing methods,[18,76] increase in nucleic acid loading density, fluorescence burst and signal recovery, real-time tracking ability, and specificity and sensitivity of the nanoprobe design. For example, AS1411 ligands are modified on DNA tetrahedral nanoprobes (apt-ADTNs) to enable specific binding to tumor cells, Q-oligo is modified from the nanoprobe to enable piRNA-36026 specific binding, and Q-oligo is modified on DNA tetrahedral

Table 5. Main application of nanoprobes and the new explorations of creative nanoprobes in the DNA area

Excitation substances	Probe type	Imaging pattern	Fluorescence signal recovery
Gao et al.[18]	COF@Survivin/MUC1	Transmission electron microscopy, scanning electron microscopy, confocal imaging	Cy5, TAMRA
microRNA-21[19]	UCNPs-NH2/PEG-DNA/FA	Fluorescence imaging	UCNP fluorescence signal
piRNA-36026[20]	Aptamer-functionalized activatable DNA tetrahedral nanoprobes (APT-ADTNs)	Confocal fluorescence imaging	Cy5 of APT-ADTNS
PH, protein[26]	AuNP-IAQs	Confocal microscopy imaging, which can also image MUC1 protein *in situ* on the surface of living cells	Cy5
Survivin[21]	M-BQD	Ratiometric fluorescence imaging	M-BQD
APE-1, TE[22]	MGB-BHQ-DNA	Confocal microscopy imaging	By cleaving APE1
ATP[23]	DNA nanoprobes exposed to Mn2+ and split aptazyme probes	Confocal imaging, fluorescence images of live mice acquired at different time points with the IVIS imaging system	Fluorescein isothiocyanate (FITC) (excitation/emission wavelengths of 488/517 nm) and cyanine-5 (Cy5) (excitation/emission wavelengths of 633/670 nm)

DNA probes are mainly used for intracellular imaging, and the cells used in the development of the probes are MCF-7 cells. The exploration of DNA probes provides new explorations for the implementation of subcellular structural localization and even genetic diagnosis in the future clinic, which is currently being attempted by researchers. We summarize the imaging techniques used for DNA nanoprobes in the last 5 years, the biomarkers of staining, and the application of high-resolution imaging *in vivo*. COF@Survivin/MUC1 nanoprobes adsorbed on functional nucleic acids, a Cy5-labeled MUC1 aptamer and a TAMRA-labeled survivin mRNA antisense oligonucleotide, UCNPs-NH2/PEG-DNA/FA, Upon attachment of double-stranded DNA to the surface of UCNPS-NH2/PEG nanocomposites, APT-ADTns have the advantages of low cell permeability, low cytotoxicity, and high resistance to enzymatic degradation. Intracellular probes. AuNP-IAQs is an integrated dual-response probe that is biocompatible and biostable, responding to acidity changes from pH 7.4 to pH 6.5, sensitively and selectively recognizing, and imaging target proteins *in situ* on the surface of living cells. M-BQD is single-stranded DNA complementary to the base sequence of survivin mRNA that can be used to target tumor cells. MGB-BHQ-DNA can avoid mutual interference and background noise and ensure enhanced fluorescence signal output during dual enzyme catalysis. All the cell lines the experiments applied are MCF-7/MCF-10, except for AuNP-IAQs, which also use HepG2 cells to better detect PH levels.

nanoprobes, binding and enabling piRNA-36026 to specifically bind and Q-oligo to detach from the nanoprobes, leading to the recovery of Cy5 fluorescence signal. There are also studies designing specific split-type nanoprobes[18,20,23,77] using glutathione, where the MnO2 nanocarrier is degraded in the presence of GSH, releasing Mn2+ ions and split-type aptazyme probes. Intracellular ATP then triggers the formation of integrative aptazyme, which activates the catalytic reaction of DNAzyme, thereby specifically lighting up tumor cells. There are also probes of different designs, such as those realized on nanoscale fluorescent COFs by adsorbing TAMRA-labeled survivin mRNA antisense nucleotides and Cy5-labeled transmembrane glycoprotein MUC1 (mucin 1) aptamers.[18,20,23,77] Furthermore, according to Wang et al., DNA nanoprobes have its own structure evolutionary history, from 1D (nanowire shape[78]) and 2D (tiles,[79] DNA origami, which sounds like a delicate and sophisticated work,[80,81] Starpattern[82]) to 3D (cube, tetrahedron/octahedron, prism, nanorobot, hydrogel, nanoflowers, DNA network).

SERS NANOPROBE

Raman imaging represents a cutting-edge advancement in surface-scanning laser Raman technology, seamlessly integrating microscopy principles with laser Raman spectroscopy. Characterized by high-speed operation, noninvasiveness, label-free capabilities, and exceptional resolution, it offers a novel approach to imaging.[83] Regarding Raman scattering fluorescent nanoprobes, which are more applied to the single-cell field,[84] Zhang et al. engineered a nanoparticle composed of gold-nucleated-4-mercaptobenzonitrile-silver-shell-goat-anti-rabbit-immunoglobulin G (Au@4-MBN@Ag@IgG) nanoparticles, which serves as an SERS nanoprobe. This nanoprobe demonstrates efficacy in detecting the HERG ion channel at the single-cell level.[84] Additionally, pH SERS probes are constructed using sensitive molecules primarily comprising carboxyl, amino, and pyridine rings with pH responsiveness. Among the most notable signaling molecules utilized are 4-mercaptobenzoic acid (4-MBA), 4-mercaptopurine (4-MPY), and p-aminophenyl thiol (4-ATP).[83,85–87] Lin et al. developed a bimodal nanoprobe designed for detecting the BAX mRNA gene. As the probe approached the sequence modified by this apoptotic site, the SERS signal was attenuated while the fluorescence signal was intensified, leading to successful differentiation from normal tissues.[88] Lin et al. discovered that ultrafine Fe3O4 nanoparticles exhibit excellent SERS activity. These nanoparticles possess narrow forbidden bandwidths and high densities of electronic states (DOS), facilitating the formation of stable ultrasmall-molecule Fe3O4-SERS molecular systems and strong coupling and resonance. These factors synergistically endow ultrasmall Fe3O4 nanoparticles with an efficient photo-induced charge transfer (PICT) process, amplifying the molecule's polarization tensor and resulting in significantly enhanced Raman signals.[89] Pure Fe3O4-based probes were employed as T1 magnetic resonance

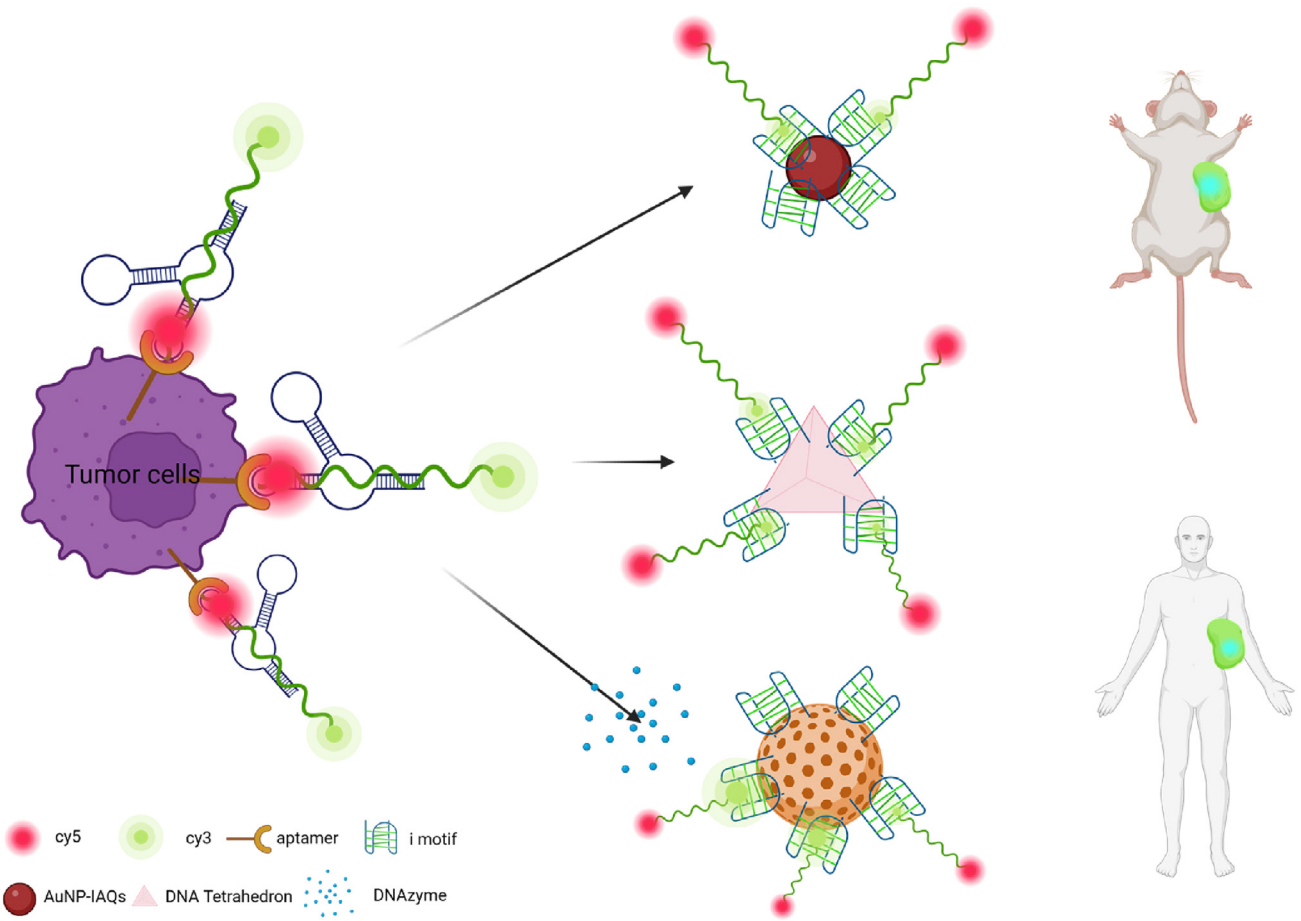

Figure 5. The description of the structure of DNA nanoprobes

contrast agents for *in vivo* tumor imaging, facilitating effective tumor diagnostics through SERS-MRI dual-mode imaging at both cellular and tissue levels. The optimized SERS-MRI bimodal nanoprobes hold promise for widespread application in early tumor diagnosis, both *in vivo* and *in vitro*, and exhibit significant potential for utilization in image-guided tumor therapy.

The probes delineated in the present study encompass gold nanoparticles, silver nanoparticles, hybrid nanoparticles, carbon-based nanomaterials coordinated with metals, and black phosphorus-based nanomaterials coordinated with metals.[90] Given the robust localized surface plasmon resonance (LSPR) exhibited by gold nanoparticle probes, Au SERS nanoprobes currently stand as the foremost choice, boasting enhanced imaging prowess even at the microscopic scale. Leveraging these nanoprobes for binding with molecular markers on cellular surfaces facilitates the generation of potent Raman signals.[84,89,91] Raman signaling molecules adhere to the probe via chemical bonding and physical adsorption mechanisms. However, both modes exhibit inherent instabilities. Consequently, researchers have delved into diverse material structural designs and modes to address these challenges. Among these explorations, Li et al. pioneered the development of an Au-Se SERS probe, demonstrating significant enhancements in bonding modalities and stability compared to conventional approaches.[89] Au always combined with SERS nanoprobes because of its outstanding advantages.[92–98] Table 6 shows the new advances in SERS probe technology in the last 5 years. Explorations into achieving superior intracellular imaging, characterized by intensified Raman signals, have extended beyond nanomaterials to encompass enhancements in physical conditions and related factors. In this vein, Zhang et al. innovatively devised a strategy involving the integration of a 4-NBT Raman reporter within an electromagnetic hotspot termed P-GERT. This design capitalizes on internal nano-GaP entities positioned at nucleus-shell junctions and external nano-GaP constituents arranged in a petal-like shell structure. The resulting configuration enables high-speed and high-contrast bioimaging of cells and tissues.[99] Zheng et al. have pioneered a novel small molecule detection methodology leveraging two distinct signaling mechanisms: SERS peak intensity and peak displacement. This innovative approach, termed INSPIRE assay, integrates 3D printing for precise delineation of the plasma substrate. The INSPIRE assay offers an optical biosensing strategy characterized by high throughput, scalability, efficiency, and immunity to cross-talk. Its implementation holds promise for enabling future clinical tests, including enzyme-linked immunosorbent assay (ELISA), to offer novel solutions.[100]

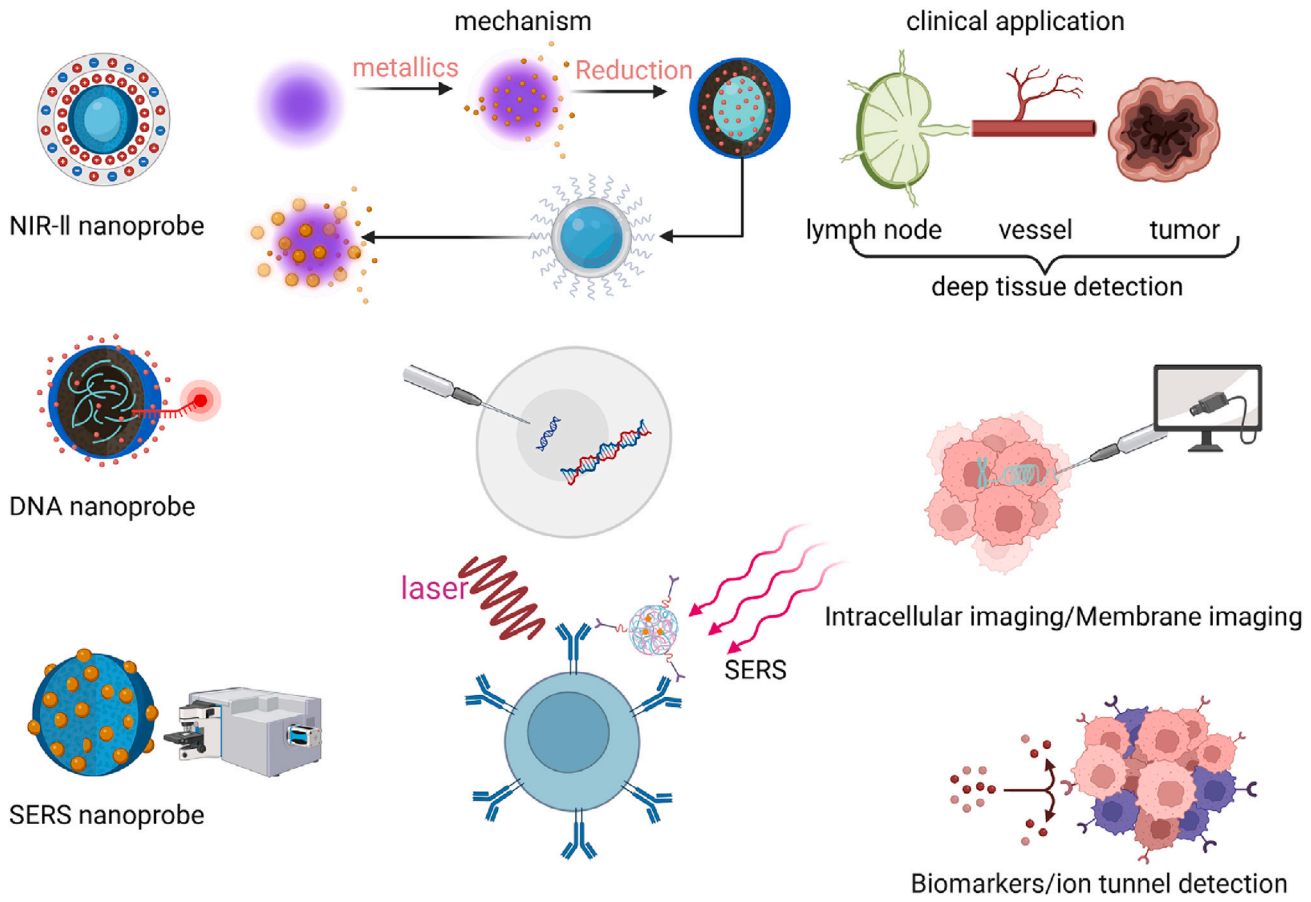

Figure 6. Comparison of three nanoprobes

CONCLUSION

In conclusion, the application of nanoprobes for *in vivo* high-resolution imaging holds significant promise for the future of biomedical research and clinical practice. Throughout this review, we have meticulously examined and synthesized the utilization of nanoprobes in three key areas: NIR spectroscopy, SERS Raman spectroscopy, and DNA functional probes for intracellular imaging (Figure 6). These modalities represent cutting-edge technologies that are currently the focus of intense research and development efforts.

However, the translation of these technologies into consistent and effective clinical applications poses several challenges. One such challenge lies in achieving uniformity in fluorescence imaging directionality across different types of probes. This necessitates advancements not only in probe design and synthesis but also in the development of standardized protocols for probe administration and imaging protocols.

Regarding the comparison of the three types of nano-fluorescent probes, first of all, putting aside the probe technology, the clinical technology that is widely used is ICG fluorescent dye This technology is used for surgical navigation to determine the site of the tumor. DNA nanoprobes are more confined to the cellular and subcellular level of the basic research,[22,25,107–109] and Raman spectroscopy is currently used in the clinical diagnosis of pathological area.[90,110–112] Therefore, in the future direction of nanoprobes, the application areas of these three kinds of probes may also tend to be clinical diagnosis, pathological diagnosis, and drug delivery and release. ICG has been widely used in surgical navigation, and in future NIR nanoprobes are more hopeful to be used in more sophisticated clinical diagnosis, surgical operations, drug delivery, and so on and in all nanoprobe materials. We are prone to think that gold nanoprobes are more likely to be used to determine the location of tumors. We tend to believe that gold nanoprobes cause the least damage to patients. Still, they also have many disadvantages: for example, expensive cost, which is also an aspect we need to consider, whereas DNA nanoprobes may tend to be used for basic research in the clinic, as well as genetic diagnosis, etc., and SERS probes are expected to maximize their value in the process of pathological diagnosis in the future. There is no way to say which probe is more suitable for clinical use, but we can only say that these three kinds of nanoprobes are expected to play their greatest value in various fields in the clinic.

Furthermore, the process of evaluating the safety and efficacy of nanoprobes for clinical use involves comprehensive assessments of biocompatibility, tissue distribution, and metabolic pathways. This often requires the construction of relevant animal

Table 6. The main application of nanoprobes and the new explorations of creative nanoprobes in the SERS area

Au@Ag NPs[101]	HER2 biomarker detection	Breast cancer
Molybdenum-disulfide-based nanoprobes, mos2[102]	4T1 cells	Cell imaging *in vivo*
SiO2@Au@Au500 NPs[103]	HCT116	Cell imaging *in vivo*
AuNFs[90]	Hek 293 and HeLa cells According to PH	Cell imaging *in vivo*
Ag/Au NS[104]	Chemotherapeutic drugs' action on cancer cells	–
Manganese dioxide (MnO2) core and silver/gold nanoparticles (Ag/Au NPs)[105]	Glutathione (GSH)	–
Nucleotide–Au-NP–graphene[106]	Nucleotide detection	–
SERS-based boric acid nanoprobe[100]	Intracellular ROS level and PI(3,4,5)P3 content	Ginsenoside Rg3-induced cell apoptosis that participates in PI3K/Akt pathway's regulatory effect

SERS probe is a probe IVI means based on Raman spectroscopy, using the strong signal of Raman for imaging *in vivo*. At present, there are many Raman spectroscopy techniques applied to tumor diagnosis to achieve accurate diagnosis with non-invasive operation techniques, and the development of nanoprobes in the field of Raman spectroscopy still has many challenges.

models to simulate *in vivo* conditions and rigorous testing to ensure the probes' compatibility with biological systems.

In addition to these technical challenges, the sheer diversity of available nanoprobes underscores the need for systematic experimentation to identify the most suitable probes for specific biomedical applications. This requires interdisciplinary collaboration between researchers in material science, biology, and medicine to leverage their collective expertise and resources.

Despite these challenges, the ongoing advancements in nanotechnology and imaging modalities offer unprecedented opportunities for non-invasive and high-resolution visualization of biological processes in real time. By addressing the current limitations and overcoming the hurdles in clinical translation, nanoprobes have the potential to revolutionize diagnostics, therapeutics, and personalized medicine soon.

ACKNOWLEDGMENTS

Funding: None.

AUTHOR CONTRIBUTIONS

S.K. participated in the writing of the paper. H.L. participated in the writing of the paper. Y.Z. participated in the writing of the paper. J.F. participated in the writing of the paper. W.H. participated in the writing of the paper.

DECLARATION OF INTERESTS

The authors have no conflicts of interest to declare.

REFERENCES

1. Chu, B., Wang, A., Cheng, L., Chen, R., Shi, H., Song, B., Dong, F., Wang, H., and He, Y. (2021). Ex vivo and in vivo fluorescence detection and imaging of adenosine triphosphate. J. Nanobiotechnol. *19*, 187. https://doi.org/10.1186/s12951-021-00930-4.
2. Karaman, D.Ş., Sarparanta, M.P., Rosenholm, J.M., and Airaksinen, A.J. (2018). Multimodality Imaging of Silica and Silicon Materials In Vivo. Adv. Mater. *30*, e1703651. https://doi.org/10.1002/adma.201703651.
3. Teng, L., Song, G., Liu, Y., Han, X., Li, Z., Wang, Y., Huan, S., Zhang, X.B., and Tan, W. (2019). Nitric Oxide-Activated "Dual-Key-One-Lock" Nanoprobe for in Vivo Molecular Imaging and High-Specificity Cancer Therapy. J. Am. Chem. Soc. *141*, 13572–13581. https://doi.org/10.1021/jacs.9b05901.
4. Ge, X., Cui, H., Kong, J., Lu, S.Y., Zhan, R., Gao, J., Xu, Y., Lin, S., Meng, K., Zu, L., et al. (2020). A Non-Invasive Nanoprobe for In Vivo Photoacoustic Imaging of Vulnerable Atherosclerotic Plaque. Adv. Mater. *32*, e2000037. https://doi.org/10.1002/adma.202000037.
5. Ma, G., Gao, X., Jiang, C., Xing, S., Wei, C., Huang, P., and Lin, J. (2019). pH-Responsive Nanoprobe for In Vivo Photoacoustic Imaging of Gastric Acid. Anal. Chem. *91*, 13570–13575. https://doi.org/10.1021/acs.analchem.9b02701.
6. Su, Y., Ye, L., Gu, J., Zhao, L., Zhou, Y., and Peng, J. (2022). Sensing and imaging of PPi in vivo using lanthanide-based second near-infrared luminescent probes. J. Mater. Chem. B *10*, 1055–1062. https://doi.org/10.1039/d1tb02579a.
7. Chen, J., Chen, L., Wu, Y., Fang, Y., Zeng, F., Wu, S., and Zhao, Y. (2021). A H(2)O(2)-activatable nanoprobe for diagnosing interstitial cystitis and liver ischemia-reperfusion injury via multispectral optoacoustic tomography and NIR-II fluorescent imaging. Nat. Commun. *12*, 6870. https://doi.org/10.1038/s41467-021-27233-4.
8. Fan, Y., Lu, M., Yu, X.A., He, M., Zhang, Y., Ma, X.N., Kou, J., Yu, B.Y., and Tian, J. (2019). Targeted Myocardial Hypoxia Imaging Using a Nitroreductase-Activatable Near-Infrared Fluorescent Nanoprobe. Anal. Chem. *91*, 6585–6592. https://doi.org/10.1021/acs.analchem.9b00298.
9. Samanta, S., Huang, M., Li, S., Yang, Z., He, Y., Gu, Z., Zhang, J., Zhang, D., Liu, L., and Qu, J. (2021). AIE-active two-photon fluorescent nanoprobe with NIR-II light excitability for highly efficient deep brain vasculature imaging. Theranostics *11*, 2137–2148. https://doi.org/10.7150/thno.53780.
10. Chen, C., Zhang, X., Gao, Z., Feng, G., and Ding, D. (2024). Preparation of AIEgen-based near-infrared afterglow luminescence nanoprobes for tumor imaging and image-guided tumor resection. Nat. Protoc. *19*, 2408–2434. https://doi.org/10.1038/s41596-024-00990-4.
11. Dang, Y., Lai, Y., Chen, F., Sun, Q., Ding, C., Zhang, W., and Xu, Z. (2022). Activatable NIR-II Fluorescent Nanoprobe for Rapid Detection and Imaging of Methylglyoxal Facilitated by the Local Nonpolar Microenvironment. Anal. Chem. *94*, 1076–1084. https://doi.org/10.1021/acs.analchem.1c04076.

12. Dunn, B., Hanafi, M., Hummel, J., Cressman, J.R., Veneziano, R., and Chitnis, P.V. (2023). NIR-II Nanoprobes: A Review of Components-Based Approaches to Next-Generation Bioimaging Probes. Bioengineering *10*, 954. https://doi.org/10.3390/bioengineering10080954.

13. Ding, C., Cheng, S., Zhang, C., Xiong, Y., Ye, M., and Xian, Y. (2019). Ratiometric Upconversion Luminescence Nanoprobe with Near-Infrared Ag(2)S Nanodots as the Energy Acceptor for Sensing and Imaging of pH in Vivo. Anal. Chem. *91*, 7181–7188. https://doi.org/10.1021/acs.analchem.9b00404.

14. Peng, L., Liu, Y., Zhang, J., Zhang, Z., Liu, Z., Fang, X., Wang, Y., and Wu, C. (2022). Surface Plasmon-Enhanced NIR-II Fluorescence in a Multilayer Nanoprobe for Through-Skull Mouse Brain Imaging. ACS Appl. Mater. Interfaces *14*, 38575–38583. https://doi.org/10.1021/acsami.2c11218.

15. Liang, M., Hu, Q., Yi, S., Chi, Y., and Xiao, Y. (2023). Development of an Au nanoclusters based activatable nanoprobe for NIR-II fluorescence imaging of gastric acid. Biosens. Bioelectron. *224*, 115062. https://doi.org/10.1016/j.bios.2023.115062.

16. Gu, Y., Zhou, Y., Wu, Y., Ma, J., Wang, Y., Wang, Q., and Wang, Y. (2021). Apoferritin-Engineered Nanoprobe for Tumor-Targeted Triple-NIR Imaging and Phototherapy. Anal. Chem. *93*, 8835–8845. https://doi.org/10.1021/acs.analchem.1c00730.

17. Wang, X., Dai, G., Jiang, G., Zhang, D., Wang, L., Zhang, W., Chen, H., Cheng, T., Zhou, Y., Wei, X., et al. (2023). A TMVP1-modified near-infrared nanoprobe: molecular imaging for tumor metastasis in sentinel lymph node and targeted enhanced photothermal therapy. J. Nanobiotechnol. *21*, 130. https://doi.org/10.1186/s12951-023-01883-6.

18. Gao, P., Wei, R., Chen, Y., Liu, X., Zhang, J., Pan, W., Li, N., and Tang, B. (2021). Multicolor Covalent Organic Framework-DNA Nanoprobe for Fluorescence Imaging of Biomarkers with Different Locations in Living Cells. Anal. Chem. *93*, 13734–13741. https://doi.org/10.1021/acs.analchem.1c03545.

19. Gong, Y., Yuan, W., Song, F., Zhang, Q., Zhang, P., and Ding, C. (2022). A NIR light gated targeting nanoprobe based on DNA-modified upconversion nanoparticles with antifouling properties for ratiometric detection and imaging of microRNA-21. Anal. Chim. Acta *1235*, 340554. https://doi.org/10.1016/j.aca.2022.340554.

20. Jia, R., He, X., Ma, W., Lei, Y., Cheng, H., Sun, H., Huang, J., and Wang, K. (2019). Aptamer-Functionalized Activatable DNA Tetrahedron Nanoprobe for PIWI-Interacting RNA Imaging and Regulating in Cancer Cells. Anal. Chem. *91*, 15107–15113. https://doi.org/10.1021/acs.analchem.9b03819.

21. Lin, P., Zhang, L., Chen, D., Xu, J., Bai, Y., and Zhao, S. (2021). A DNA-functionalized biomass nanoprobe for the targeted photodynamic therapy of tumor and ratiometric fluorescence imaging-based visual cancer cell identification/antitumor drug screening. Analyst *146*, 835–841. https://doi.org/10.1039/d0an02006k.

22. Zeng, Z., Guo, B., Li, X., Fu, X., Chen, Y., Wu, H., Zhang, L., Chen, J., and Ding, S. (2022). A simple and smart AND-gate DNA nanoprobe for correlated enzymes tracking and cell-selective imaging. Biosens. Bioelectron. *217*, 114724. https://doi.org/10.1016/j.bios.2022.114724.

23. Zhou, Y., Zou, L., Li, G., Shi, T., Yu, S., Wang, F., and Liu, X. (2021). A Cooperatively Activatable DNA Nanoprobe for Cancer Cell-Selective Imaging of ATP. Anal. Chem. *93*, 13960–13966. https://doi.org/10.1021/acs.analchem.1c03284.

24. Ji, X., Wang, Z., Niu, S., and Ding, C. (2020). DNAzyme-functionalized porous carbon nanospheres serve as a fluorescent nanoprobe for imaging detection of microRNA-21 and zinc ion in living cells. Mikrochim. Acta *187*, 249. https://doi.org/10.1007/s00604-020-04226-6.

25. Wu, X., Shuai, X., Nie, K., Li, J., Liu, L., Wang, L., Huang, C., and Li, C. (2024). DNA-Based Fluorescent Nanoprobe for Cancer Cell Membrane Imaging. Molecules *29*, 267. https://doi.org/10.3390/molecules29010267.

26. Kan, A., Wang, S., Zhang, L., Xu, X., Zhang, N., and Jiang, W. (2021). A functional DNA-modified dual-response gold nanoprobe for simultaneously imaging the acidic microenvironment and membrane proteins of tumor cells. Talanta *229*, 122284. https://doi.org/10.1016/j.talanta.2021.122284.

27. Wu, Z., Tang, Y., Chen, L., Liu, L., Huo, H., Ye, J., Ge, X., Su, L., Chen, Z., and Song, J. (2022). In-Situ Assembly of Janus Nanoprobe for Cancer Activated NIR-II Photoacoustic Imaging and Enhanced Photodynamic Therapy. Anal. Chem. *94*, 10540–10548. https://doi.org/10.1021/acs.analchem.2c02108.

28. Yao, D., Wang, Y., Zou, R., Bian, K., Liu, P., Shen, S., Yang, W., Zhang, B., and Wang, D. (2020). Molecular Engineered Squaraine Nanoprobe for NIR-II/Photoacoustic Imaging and Photothermal Therapy of Metastatic Breast Cancer. ACS Appl. Mater. Interfaces *12*, 4276–4284. https://doi.org/10.1021/acsami.9b20147.

29. Dong, J., Sun, J., Cai, W., Guo, C., Wang, Q., Zhao, X., and Zhang, R. (2022). A natural cuttlefish melanin nanoprobe for preoperative and intraoperative mapping of lymph nodes. Nanomedicine. *41*, 102510. https://doi.org/10.1016/j.nano.2021.102510.

30. Fan, X., Li, Y., Feng, Z., Chen, G., Zhou, J., He, M., Wu, L., Li, S., Qian, J., and Lin, H. (2021). Nanoprobes-Assisted Multichannel NIR-II Fluorescence Imaging-Guided Resection and Photothermal Ablation of Lymph Nodes. Adv. Sci. *8*, 2003972. https://doi.org/10.1002/advs.202003972.

31. Wang, Y., Zhang, W., Sun, P., Cai, Y., Xu, W., Fan, Q., Hu, Q., and Han, W. (2019). A Novel Multimodal NIR-II Nanoprobe for the Detection of Metastatic Lymph Nodes and Targeting Chemo-Photothermal Therapy in Oral Squamous Cell Carcinoma. Theranostics *9*, 391–404. https://doi.org/10.7150/thno.30268.

32. Yang, Z., Ji, Y., Jia, Q., Feng, Y., Ji, R., Bai, M., Yan, H., Sun, F., Zhang, R., and Wang, Z. (2024). Real-time detection and resection of sentinel lymph node metastasis in breast cancer through a rare earth nanoprobe based NIR-IIb fluorescence imaging. Mater. Today. Bio *28*, 101166. https://doi.org/10.1016/j.mtbio.2024.101166.

33. Liu, S., Xu, W., Li, X., Pang, D.W., and Xiong, H. (2022). BOIMPY-Based NIR-II Fluorophore with High Brightness and Long Absorption beyond 1000 nm for In Vivo Bioimaging: Synergistic Steric Regulation Strategy. ACS Nano *16*, 17424–17434. https://doi.org/10.1021/acsnano.2c08619.

34. Meng, J., Feng, Z., Qian, S., Wang, C., Li, X., Gao, L., Ding, Z., Qian, J., and Liu, Z. (2022). Mapping physiological and pathological functions of cortical vasculature through aggregation-induced emission nanoprobes assisted quantitative, in vivo NIR-II imaging. Biomater. Adv. *136*, 212760. https://doi.org/10.1016/j.bioadv.2022.212760.

35. Morales-Conde, S., Licardie, E., Alarcón, I., and Balla, A. (2022). Indocyanine green (ICG) fluorescence guide for the use and indications in general surgery: recommendations based on the descriptive review of the literature and the analysis of experience. Cirugía Española (English Edition) *100*, 534–554. https://doi.org/10.1016/j.cireng.2022.06.023.

36. Bi, S., Deng, Z., Jiang, Q., Jiang, M., and Zeng, S. (2021). A H(2)S-Triggered Dual-Modal Second Near-Infrared/Photoacoustic Intelligent Nanoprobe for Highly Specific Imaging of Colorectal Cancer. Anal. Chem. *93*, 13212–13218. https://doi.org/10.1021/acs.analchem.1c02200.

37. Asha Krishnan, M., Yadav, K., Roach, P., and Chelvam, V. (2021). A targeted near-infrared nanoprobe for deep-tissue penetration and imaging of prostate cancer. Biomater. Sci. *9*, 2295–2312. https://doi.org/10.1039/d0bm01970d.

38. Shi, X., Xu, P., Cao, C., Cheng, Z., Tian, J., and Hu, Z. (2022). PET/NIR-II fluorescence imaging and image-guided surgery of glioblastoma using a folate receptor α-targeted dual-modal nanoprobe. Eur. J. Nucl. Med. Mol. Imaging *49*, 4325–4337. https://doi.org/10.1007/s00259-022-05890-x.

39. Wang, R., Shi, J., Zhang, Q., Peng, Q., Sun, X., Song, L., and Zhang, Y. (2023). Dual-Triggered Near-Infrared Persistent Luminescence Nanoprobe for Autofluorescence-Free Imaging-Guided Precise Therapy of Rheumatoid Arthritis. Adv. Sci. *10*, e2205320. https://doi.org/10.1002/advs.202205320.

40. Wei, T., Xing, H., Wang, H., Zhang, Y., Wang, J., Shen, J., and Dai, Z. (2020). Bovine serum albumin encapsulation of near infrared fluorescent nano-probe with low nonspecificity and cytotoxicity for imaging of HER2-positive breast cancer cells. Talanta *210*, 120625. https://doi.org/10.1016/j.talanta.2019.120625.

41. Jiang, D., Tan, Q., Shen, Y., Ye, M., Li, J., and Zhou, Y. (2023). NIR-excited imaging and in vivo visualization of β-galactosidase activity using a pyranonitrile-modified upconversion nanoprobe. Spectrochim. Acta Mol. Biomol. Spectrosc. *292*, 122411. https://doi.org/10.1016/j.saa.2023.122411.

42. Shiqi, W., Bowen, L., Jicheng, Y., and Zhen, G. (2022). Near-infrared-II Fluorescence Imaging for Tumor Diagnosis and Therapy. Chem. J. Chin. Univ. *43*, 20220577. https://doi.org/10.7503/cjcu20220577.

43. Zhu, Y.Y., Song, L., Zhang, Y.Q., Liu, W.L., Chen, W.L., Gao, W.L., Zhang, L.X., Wang, J.Z., Ming, Z.H., Zhang, Y., and Zhang, G.J. (2023). Development of a Rare Earth Nanoprobe Enables In Vivo Real-Time Detection of Sentinel Lymph Node Metastasis of Breast Cancer Using NIR-IIb Imaging. Cancer Res. *83*, 3428–3441. https://doi.org/10.1158/0008-5472.Can-22-3432.

44. Zhao, M., Ding, J., Mao, Q., Zhang, Y., Gao, Y., Ye, S., Qin, H., and Shi, H. (2020). A novel α v β 3 integrin-targeted NIR-II nanoprobe for multimodal imaging-guided photothermal therapy of tumors in vivo. Nanoscale *12*, 6953–6958.

45. Chen, J., Chen, L., Zeng, F., and Wu, S. (2022). Aminopeptidase N Activatable Nanoprobe for Tracking Lymphatic Metastasis and Guiding Tumor Resection Surgery via Optoacoustic/NIR-II Fluorescence Dual-Mode Imaging. Anal. Chem. *94*, 8449–8457. https://doi.org/10.1021/acs.analchem.2c01241.

46. Liu, J., Li, M., Dang, Y., Lou, H., Xu, Z., and Zhang, W. (2022). NIR-I fluorescence imaging tumorous methylglyoxal by an activatable nanoprobe based on peptide nanotubes by FRET process. Biosens. Bioelectron. *204*, 114068. https://doi.org/10.1016/j.bios.2022.114068.

47. Zhao, X., Zhang, L., Gao, W., Yu, X., Gu, W., Fu, W., and Luo, Y. (2020). Spatiotemporally Controllable MicroRNA Imaging in Living Cells via a Near-Infrared Light-Activated Nanoprobe. ACS Appl. Mater. Interfaces *12*, 35958–35966. https://doi.org/10.1021/acsami.0c10962.

48. Guo, H., and Miao, Y. (2012). Cu-64-labeled lactam bridge-cyclized α-MSH peptides for PET imaging of melanoma. Mol. Pharm. *9*, 2322–2330. https://doi.org/10.1021/mp300246j.

49. Qiao, Z., Xu, J., Gonzalez, R., and Miao, Y. (2022). Novel (64)Cu-Labeled NOTA-Conjugated Lactam-Cyclized Alpha-Melanocyte-Stimulating Hormone Peptides with Enhanced Tumor to Kidney Uptake Ratios. Mol. Pharm. *19*, 2535–2541. https://doi.org/10.1021/acs.molpharmaceut.2c00211.

50. Prasanphanich, A.F., Nanda, P.K., Rold, T.L., Ma, L., Lewis, M.R., Garrison, J.C., Hoffman, T.J., Sieckman, G.L., Figueroa, S.D., and Smith, C.J. (2007). [64Cu-NOTA-8-Aoc-BBN(7-14)NH2] targeting vector for positron-emission tomography imaging of gastrin-releasing peptide receptor-expressing tissues. Proc. Natl. Acad. Sci. USA *104*, 12462–12467. https://doi.org/10.1073/pnas.0705347104.

51. Ait-Mohand, S., Fournier, P., Dumulon-Perreault, V., Kiefer, G.E., Jurek, P., Ferreira, C.L., Bénard, F., and Guérin, B. (2011). Evaluation of 64Cu-labeled bifunctional chelate-bombesin conjugates. Bioconjug. Chem. *22*, 1729–1735. https://doi.org/10.1021/bc2002665.

52. Boswell, C.A., Sun, X., Niu, W., Weisman, G.R., Wong, E.H., Rheingold, A.L., and Anderson, C.J. (2004). Comparative in vivo stability of copper-64-labeled cross-bridged and conventional tetraazamacrocyclic complexes. J. Med. Chem. *47*, 1465–1474. https://doi.org/10.1021/jm030383m.

53. Pierce, J.T., Cho, S.S., Nag, S., Zeh, R., Jeon, J., Holt, D., Durham, A., Nasrallah, M.P., Singhal, S., and Lee, J.Y.K. (2019). Folate Receptor Overexpression in Human and Canine Meningiomas-Immunohistochemistry and Case Report of Intraoperative Molecular Imaging. Neurosurgery *85*, 359–368. https://doi.org/10.1093/neuros/nyy356.

54. Chi, Y., Hu, Q., Yi, S., Qu, H., and Xiao, Y. (2023). A novel strategy to construct activatable silver chalcogenide quantum dots nanoprobe for NIR-II fluorescence imaging of hypochlorous acid in vivo. Talanta *262*, 124668. https://doi.org/10.1016/j.talanta.2023.124668.

55. Deng, Z., Bi, S., Jiang, M., and Zeng, S. (2021). Endogenous H(2)S-Activated Orthogonal Second Near-Infrared Emissive Nanoprobe for In Situ Ratiometric Fluorescence Imaging of Metformin-Induced Liver Injury. ACS Nano *15*, 3201–3211. https://doi.org/10.1021/acsnano.0c09799.

56. Frederiks, C.N., Overwater, A., Bergman, J.J.G.H.M., Pouw, R.E., de Keizer, B., Bennink, R.J., Brosens, L.A.A., Meijer, S.L., van Hillegersberg, R., van Berge Henegouwen, M.I., et al. (2023). Feasibility and Safety of Tailored Lymphadenectomy Using Sentinel Node-Navigated Surgery in Patients with High-Risk T1 Esophageal Adenocarcinoma. Ann. Surg Oncol. *30*, 4002–4011. https://doi.org/10.1245/s10434-023-13317-6.

57. Brouwer, O.R., van den Berg, N.S., Mathéron, H.M., Wendler, T., van der Poel, H.G., Horenblas, S., Valdés Olmos, R.A., and van Leeuwen, F.W.B. (2014). Feasibility of intraoperative navigation to the sentinel node in the groin using preoperatively acquired single photon emission computerized tomography data: transferring functional imaging to the operating room. J. Urol. *192*, 1810–1816. https://doi.org/10.1016/j.juro.2014.03.127.

58. Overwater, A., Weusten, B.L.A.M., Ruurda, J.P., van Hillegersberg, R., Bennink, R.J., de Keizer, B., Meijer, S.L., Brosens, L.A.A., Pouw, R.E., Bergman, J.J.G.H.M., et al. (2022). Feasibility of sentinel node navigated surgery in high-risk T1b esophageal adenocarcinoma patients using a hybrid tracer of technetium-99 m and indocyanine green. Surg. Endosc. *36*, 2671–2679. https://doi.org/10.1007/s00464-021-08551-6.

59. Wang, Q., Li, X., Qian, B., Hu, K., and Liu, B. (2022). Fluorescence imaging in the surgical management of liver cancers: Current status and future perspectives. Asian J. Surg. *45*, 1375–1382. https://doi.org/10.1016/j.asjsur.2021.08.063.

60. KleinJan, G.H., van den Berg, N.S., van Oosterom, M.N., Wendler, T., Miwa, M., Bex, A., Hendricksen, K., Horenblas, S., and van Leeuwen, F.W.B. (2016). Toward (Hybrid) Navigation of a Fluorescence Camera in an Open Surgery Setting. J. Nucl. Med. *57*, 1650–1653. https://doi.org/10.2967/jnumed.115.171645.

61. Zhan, R., Li, X., Guo, W., Liu, X., Liu, Z., Xu, K., and Tang, B. (2019). An Aptamer-Based Near-Infrared Fluorescence Nanoprobe for Detecting and Imaging of Phospholamban Micropeptide in Cardiomyocytes. ACS Sens. *4*, 733–739. https://doi.org/10.1021/acssensors.9b00026.

62. Zheng, X., Kankala, R.K., Liu, C.-G., Wang, S.-B., Chen, A.-Z., and Zhang, Y. (2021). Lanthanides-doped near-infrared active upconversion nanocrystals: Upconversion mechanisms and synthesis. Coord. Chem. Rev. *438*, 213870. https://doi.org/10.1016/j.ccr.2021.213870.

63. Zhu, L., Ye, C., Dai, G., Wang, X., Yu, X., Liu, T., and Tao, X. (2020). Highly-efficient upconversion via direct one-photon absorption of xanthene-based chromophores. Dyes Pigments *172*, 107853. https://doi.org/10.1016/j.dyepig.2019.107853.

64. Liu, Y., Su, Q., Zou, X., Chen, M., Feng, W., Shi, Y., and Li, F. (2016). Near-infrared in vivo bioimaging using a molecular upconversion probe. Chem. Commun. *52*, 7466–7469.

65. Wei, Z., Duan, G., Huang, B., Qiu, S., Zhou, D., Zeng, J., Cui, J., Hu, C., Wang, X., Wen, L., and Gao, M. (2021). Rapidly liver-clearable rare-earth core–shell nanoprobe for dual-modal breast cancer imaging in the second near-infrared window. J. Nanobiotechnol. *19*, 369.

66. Zhu, Y., Luo, X., Yu, Z., Wen, S., Bao, G., Zhang, L., Zhang, C., and Xian, Y. (2023). Dye-sensitized rare-earth-doped nanoprobe for simultaneously enhanced NIR-II imaging and precise treatment of bacterial infection. Acta Biomater. *170*, 532–542.

67. Zheng, X., Cui, L., Chen, M., Soto, L.A., Graves, E.E., and Rao, J. (2019). A near-infrared phosphorescent nanoprobe enables quantitative, longitudinal imaging of tumor hypoxia dynamics during radiotherapy. Cancer Res. *79*, 4787–4797.

68. Luo, R., Ou, C., Li, X., Wang, Y., Du, W., Liang, G., and Gong, C. (2022). An acidity-initiated self-assembly/disassembly nanoprobe to switch on fluorescence for tumor-targeted near-infrared imaging. Nano Lett. *22*, 151–156.

69. Wang, W., Fang, Z., Zhang, X., Cai, H., Zhao, Y., Gu, W., Yang, X., and Wu, Y. (2020). A Self-Assembled "Albumin–Conjugate" Nanoprobe for Near Infrared Optical Imaging of Subcutaneous and Metastatic Tumors. ACS Appl. Bio Mater. *3*, 327–334.

70. Zhao, Y.-T., Chen, X.-X., Jiang, W.-L., Li, Y., Fei, J., and Li, C.-Y. (2020). Near-infrared fluorescence MOF nanoprobe for adenosine triphosphate-guided imaging in colitis. ACS Appl. Mater. Interfaces *12*, 47840–47847.

71. Xia, X., Hao, Y., Hu, S., and Wang, J. (2014). Hairpin DNA probe with 5′-TCC/CCC-3′ overhangs for the creation of silver nanoclusters and miRNA assay. Biosens. Bioelectron. *51*, 36–39.

72. Miao, X., Mao, R., You, Y., Zhou, H., Qiu, C., Li, X., Chen, Z., Ren, J., Chen, M., Wang, P., et al. (2021). Intracolic ultrasound molecular imaging: a novel method for assessing colonic tumor necrosis factor-α expression in inflammatory bowel disease. Mol. Med. *27*, 119.

73. Peng, P., Wang, Q., Du, Y., Wang, H., Shi, L., and Li, T. (2020). Extracellular ion-responsive logic sensors utilizing DNA dimeric nanoassemblies on cell surface and application to boosting AS1411 internalization. Anal. Chem. *92*, 9273–9280.

74. Deng, Z., Gao, P., Liu, H., He, Y., Zhong, S., and Yang, Y. (2021). Cell-Surface-anchored DNA sensors for simultaneously monitoring extracellular sodium and potassium levels. Anal. Chem. *93*, 16432–16438.

75. Fan, M., Huang, H., Xu, Y., Wang, S., Chen, S., Luo, Z., and Xu, J. (2023). mRNA-activated DNAzyme nanoprobe for tumor cell precise imaging and gene therapy. Anal. Methods *15*, 4114–4118.

76. Gao, P., Yin, J., Wang, M., Wei, R., Pan, W., Li, N., and Tang, B. (2022). COF-DNA Bicolor Nanoprobes for Imaging Tumor-Associated mRNAs in Living Cells. Anal. Chem. *94*, 13293–13299. https://doi.org/10.1021/acs.analchem.2c03658.

77. Lei, Y., Tang, J., Shi, H., Ye, X., He, X., Xu, F., Yan, L., Qiao, Z., and Wang, K. (2016). Nature-Inspired Smart DNA Nanodoctor for Activatable In Vivo Cancer Imaging and In Situ Drug Release Based on Recognition-Triggered Assembly of Split Aptamer. Anal. Chem. *88*, 11699–11706. https://doi.org/10.1021/acs.analchem.6b03283.

78. Wei, Q., Huang, J., Li, J., Wang, J., Yang, X., Liu, J., and Wang, K. (2018). A DNA nanowire based localized catalytic hairpin assembly reaction for microRNA imaging in live cells. Chem. Sci. *9*, 7802–7808. https://doi.org/10.1039/c8sc02943a.

79. Fu, T.J., and Seeman, N.C. (1993). DNA double-crossover molecules. Biochemistry *32*, 3211–3220. https://doi.org/10.1021/bi00064a003.

80. Dey, S., Fan, C., Gothelf, K.V., Li, J., Lin, C., Liu, L., Liu, N., Nijenhuis, M.A.D., Saccà, B., Simmel, F.C., et al. (2021). DNA origami. Nat. Rev. Methods Primers *1*, 13. https://doi.org/10.1038/s43586-020-00009-8.

81. Hong, F., Zhang, F., Liu, Y., and Yan, H. (2017). DNA Origami: Scaffolds for Creating Higher Order Structures. Chem. Rev. *117*, 12584–12640. https://doi.org/10.1021/acs.chemrev.6b00825.

82. Kwon, P.S., Ren, S., Kwon, S.J., Kizer, M.E., Kuo, L., Xie, M., Zhu, D., Zhou, F., Zhang, F., Kim, D., et al. (2020). Designer DNA architecture offers precise and multivalent spatial pattern-recognition for viral sensing and inhibition. Nat. Chem. *12*, 26–35. https://doi.org/10.1038/s41557-019-0369-8.

83. Zhang, L., Zhao, Q., Jiang, Z., Shen, J., Wu, W., Liu, X., Fan, Q., and Huang, W. (2021). Recent progress of SERS nanoprobe for pH detecting and its application in biological imaging. Biosensors *11*, 282.

84. Zhang, W.-S., Liu, X.-P., Yue, S., Wang, Y.-N., Wang, Y., and Xu, Z.-R. (2023). In-situ and amplification-free imaging of hERG ion channels at single-cell level using a unique core-molecule-shell-secondary antibody SERS nanoprobe. Talanta *253*, 123900. https://doi.org/10.1016/j.talanta.2022.123900.

85. Ma, C., and Harris, J.M. (2011). Surface-enhanced Raman spectroscopy investigation of the potential-dependent acid-base chemistry of silver-immobilized 2-mercaptobenzoic acid. Langmuir *27*, 3527–3533. https://doi.org/10.1021/la1044859.

86. Zong, S., Wang, Z., Yang, J., and Cui, Y. (2011). Intracellular pH sensing using p-aminothiophenol functionalized gold nanorods with low cytotoxicity. Anal. Chem. *83*, 4178–4183.

87. Huang, Y., Liu, W., Wang, D., Gong, Z., and Fan, M. (2020). Evaluation of the intrinsic pH sensing performance of surface-enhanced Raman scattering pH probes. Microchem. J. *154*, 104565. https://doi.org/10.1016/j.microc.2019.104565.

88. Lin, X., Li, C., Xu, S., Wang, Z., and Ma, X. (2023). SERS-fluorescence dual-mode nanoprobe for the detection and imaging of Bax mRNA during apoptosis. Mikrochim. Acta *190*, 130.

89. Li, X., Duan, X., Li, L., Ye, S., and Tang, B. (2020). An accurate and ultrasensitive SERS sensor with Au-Se interface for bioimaging and in situ quantitation. Chem. Commun. *56*, 9320–9323. https://doi.org/10.1039/d0cc02068k.

90. Li, Q., Huo, H., Wu, Y., Chen, L., Su, L., Zhang, X., Song, J., and Yang, H. (2023). Design and Synthesis of SERS Materials for In Vivo Molecular Imaging and Biosensing. Adv. Sci. *10*, e2202051. https://doi.org/10.1002/advs.202202051.

91. Cong, L., Liang, L., Cao, F., Sun, D., Yue, J., Xu, W., Liang, C., and Xu, S. (2019). Distinguishing cancer cell lines at a single living cell level via detection of sialic acid by dual-channel plasmonic imaging and by using a SERS-microfluidic droplet platform. Microchim. Acta *186*, 367.

92. Cheng, W., Tang, P., He, X., Xing, X., Liu, S., Zhang, F., Lu, X., and Zhong, L. (2021). Au/Ag composite-based SERS nanoprobe of Cr(3). Anal. Bioanal. Chem. *413*, 2951–2960. https://doi.org/10.1007/s00216-021-03228-4.

93. Farahavar, G., Abolmaali, S.S., Nejatollahi, F., Safaie, A., Javanmardi, S., Khajeh Zadeh, H., Yousefi, R., Nadgaran, H., Mohammadi-Samani, S., Tamaddon, A.M., and Ahadian, S. (2021). Single-chain antibody-decorated Au nanocages@liposomal layer nanoprobes for targeted SERS imaging and remote-controlled photothermal therapy of melanoma cancer cells. Mater. Sci. Eng. C Mater. Biol. Appl. *124*, 112086. https://doi.org/10.1016/j.msec.2021.112086.

94. Li, P., Zhou, B., Ge, M., Jing, X., and Yang, L. (2022). Metal coordination induced SERS nanoprobe for sensitive and selective detection of histamine in serum. Talanta *237*, 122913. https://doi.org/10.1016/j.talanta.2021.122913.

95. Shu, Y., Li, J., Bai, H., Liang, A., Wen, G., and Jiang, Z. (2024). A new SERS quantitative analysis method for trace malathion with recognition and catalytic amplification difunctional MOF(Tb)@Au@MIP nanoprobe. Talanta *267*, 125166. https://doi.org/10.1016/j.talanta.2023.125166.

96. Wang, L., Patskovsky, S., Gauthier-Soumis, B., and Meunier, M. (2022). Porous Au-Ag Nanoparticles from Galvanic Replacement Applied as Single-Particle SERS Probe for Quantitative Monitoring. Small *18*, e2105209. https://doi.org/10.1002/smll.202105209.

97. Wang, Y., Li, Q., Zhang, R., Tang, K., Ding, C., and Yu, S. (2020). SERS-based immunocapture and detection of pathogenic bacteria using a boronic acid-functionalized polydopamine-coated Au@Ag nanoprobe. Mikrochim. Acta *187*, 290. https://doi.org/10.1007/s00604-020-04248-0.

98. Yin, L., You, T., El-Seedi, H.R., El-Garawani, I.M., Guo, Z., Zou, X., and Cai, J. (2022). Rapid and sensitive detection of zearalenone in corn using SERS-based lateral flow immunosensor. Food Chem. *396*, 133707. https://doi.org/10.1016/j.foodchem.2022.133707.

99. Zhang, Y., Gu, Y., He, J., Thackray, B.D., and Ye, J. (2019). Ultrabright gap-enhanced Raman tags for high-speed bioimaging. Nat. Commun. *10*, 3905.

100. Zheng, P., Wu, L., Raj, P., Mizutani, T., Szabo, M., Hanson, W.A., and Barman, I. (2022). A Dual-Modal Single-Antibody Plasmonic Spectro-Immunoassay for Detection of Small Molecules. Small *18*, 2200090.

101. Verdin, A., Malherbe, C., and Eppe, G. (2021). Spatially resolved determination of the abundance of the HER2 marker in microscopic breast tumors using targeted SERS imaging. Mikrochim. Acta *188*, 288.

102. Gong, L., Feng, L., Zheng, Y., Luo, Y., Zhu, D., Chao, J., Su, S., and Wang, L. (2022). Molybdenum Disulfide-Based Nanoprobes: Preparation and Sensing Application. Biosensors *12*, 87. https://doi.org/10.3390/bios12020087.

103. Bock, S., Choi, Y.-S., Kim, M., Yun, Y., Pham, X.H., Kim, J., Seong, B., Kim, W., Jo, A., Ham, K.M., et al. (2022). Highly sensitive near-infrared SERS nanoprobes for in vivo imaging using gold-assembled silica nanoparticles with controllable nanogaps. J. Nanobiotechnol. *20*, 130.

104. Xie, M., Li, F., Gu, P., Wang, F., Qu, Z., Li, J., Wang, L., Zuo, X., Zhang, X., and Shen, J. (2019). Gold nanoflower-based surface-enhanced Raman probes for pH mapping of tumor cell microenviroment. Cell Prolif. *52*, e12618.

105. Hu, X., Quan, C., Ren, T., Zhao, L., Shen, Y., Zhu, Y., and Wang, J. (2023). MnO2 nanoparticles decorated with Ag/Au nanotags for label-based SERS determination of cellular glutathione. Mikrochim. Acta *190*, 341.

106. Zolotoukhina, T., Yamada, M., and Iwakura, S. (2021). Vibrational Spectra of Nucleotides in the Presence of the Au Cluster Enhancer in MD Simulation of a SERS Sensor. Biosensors *11*, 37. https://doi.org/10.3390/bios11020037.

107. Tian, C., Liang, G., Wang, C., He, R., Ning, K., Li, Z., Liu, R., Ma, Y., Guan, S., Deng, J., and Zhai, J. (2022). Computer simulation and design of DNA-nanoprobe for fluorescence imaging DNA repair enzyme in living cells. Biosens. Bioelectron. *211*, 114360. https://doi.org/10.1016/j.bios.2022.114360.

108. Zhong, L., Cai, S., Huang, Y., Yin, L., Yang, Y., Lu, C., and Yang, H. (2018). DNA Octahedron-Based Fluorescence Nanoprobe for Dual Tumor-Related mRNAs Detection and Imaging. Anal. Chem. *90*, 12059–12066. https://doi.org/10.1021/acs.analchem.8b02847.

109. Zhu, C., Yang, J., Zheng, J., Chen, S., Huang, F., and Yang, R. (2019). Triplex-Functionalized DNA Tetrahedral Nanoprobe for Imaging of Intracellular pH and Tumor-Related Messenger RNA. Anal. Chem. *91*, 15599–15607. https://doi.org/10.1021/acs.analchem.9b03659.

110. Dong, Y., Dong, W., Liang, X., Wang, Y.R., Xu, F., Li, L., Han, L., and Jiang, L.R. (2023). Construction and application of thrombin-activated fluorescence-SERS dual-mode optical nanoprobes. Spectrochim. Acta Mol. Biomol. Spectrosc. *293*, 122513. https://doi.org/10.1016/j.saa.2023.122513.

111. Wang, X.Y., Yang, J.Y., Wang, Y.T., Zhang, H.C., Chen, M.L., Yang, T., and Wang, J.H. (2021). M13 phage-based nanoprobe for SERS detection and inactivation of Staphylococcus aureus. Talanta *221*, 121668. https://doi.org/10.1016/j.talanta.2020.121668.

112. Zong, S., Tang, H., Yang, K., Wang, H., Wang, Z., and Cui, Y. (2020). SERS-fluorescence-superresolution triple-mode nanoprobe based on surface enhanced Raman scattering and surface enhanced fluorescence. J. Mater. Chem. B *8*, 8459–8466. https://doi.org/10.1039/d0tb01211d.